Damage detection for offshore structures using long and short-term memory networks and random decrement technique

Xingxian Bao[a,b,1], Zhichao Wang[a], Gregorio Iglesias[c,d]

[a] School of Petroleum Engineering, China University of Petroleum (East China), Qingdao, 266580, China

[b] National Engineering Laboratory of Offshore Geophysical and Exploration Equipment, China University of Petroleum (East China), Shandong, 266580, China

[c] MaREI, Environmental Research Institute & School of Engineering, University College Cork, College Road, Cork, Ireland.

[d] University of Plymouth, School of Engineering, Marine Building, Drake Circus, Plymouth PL4 8AA, United Kingdom.

Abstract

A damage detection method is presented which combines the random decrement technique (RDT) with long and short-term memory (LSTM) networks. The method uses the measured vibration response of offshore structures subjected to random excitation and is able to locate and assess the damage with accuracy, even in noisy conditions. The applicability of the proposed RDT-LSTM method is verified through a numerical example and laboratory tests. The numerical example consists of a jacket platform subjected to random wave excitation. The simulated damage cases encompass single and multiple damage locations not only on whole segments but also on local elements (one-fifth of the whole segment) of the numerical structure, with minor (1%-5%) severity, and different noise levels. RDT is applied first to process the noisy random data, and then the damage detection is carried out using LSTM. After the numerical example, the proposed method is applied to laboratory tests of a jacket platform model under random loading produced by a shaking table. Minor and major damages and their combination at different locations are discussed. Both the numerical

[1] Corresponding author.
E-mail address: baoxingxian@upc.edu.cn (X. Bao)

simulation and laboratory test show that the proposed RDT-LSTM method has an outstanding performance in structural damage detection.
Keywords: long and short-term memory networks; random decrement technique; damage detection; offshore structures

1. Introduction

Structural health monitoring (SHM) of offshore structures plays a major role in reducing the maintenance costs and guaranteeing the operation safety during their service in harsh marine environments (Nichols, 2003; Ren et al., 2006; Jahangiri et al., 2016; Haeri et al., 2017). Among the plethora of SHM methods, vibration-based methods such as global SHM methods have been widely used to determine the damage location and damage level of a structure, using damage indicators based on the measured vibration responses. Vibration-based methods can be divided into two categories, parametric and nonparametric approaches, according to whether or not the modal parameters are used to construct the damage indicators (Abdeljaber et al., 2017).

The basic principle behind the parametric methods is that the modal parameters are associated with the physical parameters of the structures. Hence, the changes of modal parameters drew from the collected vibration response data based on sensors and the data acquisition system related to the damaged and undamaged structures are used to construct the damage indicators. During the past few decades, the parametric methods have made great advances. They are typically based on natural frequency or mode shape (Ding et al., 2016; Bao et al., 2017; Ercolani et al., 2018), frequency response function (Mohan et al., 2013; Mao et al., 2018; Lin and Ng, 2018), and modal strain energy (MSE) (Ashory et al., 2017; Tan et al., 2017; Dehcheshmeh et al., 2020). In recent years, the parametric methods, especially the MSE-based methods, have often been applied for damage detection of marine structures. Li et al. (2008) proposed a cross-model cross-mode (CMCM) approach to determine the damage of offshore jacket platforms by using spatially incomplete modal data to identify the damage of individual components. Liu et al. (2014) introduced the factors of mode correction and defined a new damage indicator based on the concept of MSE to localize the damage of offshore wind turbines based on spatial incompleteness with better accuracy. Li et al. (2016) introduced frequency information into the traditional Stubbs index method. The effectiveness of the improved method for damage localization was proved by the numerical example and laboratory study of jacket platforms. A review of four typical MSE-related damage detection methods (i.e., Stubbs damage index, MSE change ratio, cross-MSE, and MSE decomposition) was presented by Wang and Xu (2019) in which the four methods for offshore platforms damage localization were compared.

As the parametric methods rely heavily on the accuracy of the modal analysis, some signal processing techniques have been proposed to overcome the problems that arise in the identification of modal parameters, e.g., mode mixing, sensitivity to noise. Hu et al. (2013) proposed the Prony based on state-space model (Prony-SS) method, which can improve the precision of the signal decomposition and avoid the shortcomings of the Prony method, such as noise sensitivity and truncation error (Liu et al., 2019(a)). Liu et al. (2020) proposed a single mode function (SMF) decomposition method to reduce the mode mixing in the Hilbert-Huang transform (HHT) for the SHM of offshore wind turbines. Bao and Shi (2019) developed the operational modal analysis procedure NExT-SLRA-CE, in which the noise elimination method (SLRA) and ambient vibration responses processing method (NExT) are combined with the modal parameters identification method (CE). However, in practice, these parametric methods still present challenges: incomplete and inaccurate modal information (Li et al., 2008), noisy measurements (Liu et al., 2019(b); Bao, et al., 2020), solution of the ill-conditioned over-determined system of linear equations (Wang et al., 2019), etc.

On the other hand, the nonparametric methods aim to construct damage indicators from the measured data of a structure based on signal processing and statistical methods instead of modal analysis. An overview of the common signal processing techniques for SHM of civil structures was given by Amezquita-Sanchez and Adeli (2016), including statistical time series (TS) models, Kalman filter (KF), wavelet transform (WT), S transform (ST)) and newer signal processing algorithms (e.g., fast S-transform, complete ensemble empirical mode decomposition (CEEMD), empirical wavelet transform (EWT)). The main advantages and disadvantages of these methods were also summarized. Asgarian et al. (2016) adopted the rate of signal energy (RSE) of wavelet packet transform based on measured accelerations as a damage index and the experimental results indicate that RSE is more sensitive to the damage location than other locations. However, the greatest difficulty of the nonparametric approaches lies in detecting the damage effectively and efficiently from the huge amount of noise-polluted online data collected by many sensors.

In the past few years, machine learning techniques have been used in numerous vibration-based structural damage detection approaches. These are divided into parametric and non-parametric methods (Avci et al., 2021). Parametric machine learning-based approaches rely on modal parameters such as natural frequencies and mode shapes as extracted features, and then the classification is performed by a well-trained classifier to assess the structural damage. Instead, non-parametric machine learning-based methods use the outputs of certain signal processing methods which extract damage-sensitive features without the need of modal analysis. The extracted features are then fed into a machine learning algorithm to perform the damage detection. The most popular methods for feature extraction are Auto-Regressive (AR) modeling (Figueiredo et al., 2011; Santos et al., 2016; Gui el al., 2017) and Principal Component Analysis (PCA) (Dackermann et al., 2010; Bandara et al., 2013; Bandara et al., 2014). However, machine learning-based structural damage detection methods depend to a great extent on the selected damage-sensitive features and classifiers. The feature extraction techniques such as modal identification, AR modeling, and PCA usually lead to considerable computational complexity and time, and the classifier needs to be tested to ensure the robustness of the machine learning methods for the damage detection, which affects the application of machine learning-based methods in real-time SHM operations (Avci et al., 2021).

Unlike machine learning, deep learning methods have a large number of hidden layers and can automatically extract features without the need for manual feature extraction (Sony et al., 2021). Nowadays, deep learning algorithms have achieved tremendous success in a variety of application domains (Alom et al., 2019), including SHM. Deep learning methods may provide a solution to the problem of the traditional nonparametric approaches, i.e., handling a large number of noise-polluted online data, due to their strong capability to deal with high-redundancy data for feature extraction. Among them, the convolutional neural network (CNN) is one of the most popular methods used for structure damage identification (Liu and Zhang, 2019; Xu et al., 2019; Zhang et al, 2019; Khodabandehlou et al., 2019; Truong et al., 2020). Compared with traditional machine learning methods, such as SVM, random forest and decision tree, CNN has obvious advantages – no need for pre- and post-processing or for extracting features manually (Abdeljaber et al., 2017), and less noise sensitivity (Lin et al., 2018).

However, most of the CNN damage identification methods are employed considering simple damage scenarios, and some of these methods make use of two-dimensional image data rather than one-dimensional time series data to determine structural damage (Bao et al., 2021). Recent studies (Abdeljaber et al., 2017; Abdeljaber et al., 2018; Avci et al., 2018; Ince et al., 2016; Kiranyaz et al., 2018) have shown that one-dimensional CNNs have advantages over two-dimensional CNNs when dealing with one-dimensional signals. One-dimensional CNNs have a compact structure (fewer hidden layers and neurons) and can learn challenging tasks with small amounts of training data. In addition, the computational complexity of one-dimensional CNNs is significantly lower than that of two-dimensional CNNs.

Long Short-Term Memory (LSTM) networks – a major branch of Recurrent Neural Networks (RNN) – are popular for temporal information processing. In recent years, LSTM has become the most modern technique for various machine learning problems, such as computer vision, time-series data prediction and natural language processing. However, LSTM networks have not received much attention in the SHM field so far. Luo et al. (2019) proposed an SHM method using the dual-tree complex wavelet enhanced convolutional LSTM network. The results of their automotive suspension experiment showed accurate prediction with high efficiency. Yang et al. (2020) proposed a CNN-LSTM method for modal frequency identification, which showed high accuracy in the tests of various materials. Zhang et al. (2020) presented a crack detection method for concrete bridge decks based on a combination of one-dimensional CNN and LSTM methods, trained by numerous images of intact and damaged structures. To date, LSTM networks have seldom been applied to damage detection of large and complex structures such as offshore platforms, bridges and high buildings, based on one-dimensional measured vibration responses. In addition, the deep learning methods for damage detection are usually sensitive to noise, and there are few researches on anti-noise procedures for damage identification based on deep learning methods under random excitation.

The random decrement technique (RDT) first proposed by Cole (1968) is an averaging technique. It is able to draw the free decaying response data from the random vibration response data of a structure under zero mean and stationary Gaussian random excitation. As it is simple and effective in processing random vibration response output and without any prior knowledge of input, the method is commonly applied to identify modal parameters for civil and offshore structures (Budipriyanto et al., 2007; Lin and Chiang, 2012; Brincker and Ventura, 2015; Feng et al., 2017). Currently, RDT has also been used for structure damage detection. Shiryayev and Slater (2008) applied statistical characters of random signatures to identify the damage of a frame structure. Elshafey et al. (2010) adopted the combined method of RDT with neural networks to detect the damage of offshore platforms under random excitation. Morsy et al. (2017) implemented multi-channel RDT to localize the damage of concrete bridge girders.

Because the RDT has the ability to extract the free decaying response from random signals in noisy conditions, and the LSTM method has a long-term memory function, which can deal well with the gradient disappearance and gradient explosion problems during the long time-series data processing, a novel approach based on the combination of RDT and LSTM is proposed in this study to determine the damage location and damage severity of a structure based on noisy random vibration response data.

The paper is organized as follows. The LSTM and RDT are briefly introduced in Sections 2 and 3, respectively. Section 4 presents the numerical study of the RDT-LSTM method for damage detection of a jacket platform subjected to random wave excitation. The simulated single and multiple minor damages on whole segments and local elements respectively are considered, as well as the noise. RDT is applied first to process the noisy random data, and then the LSTM for damage detection is carried out utilizing the processed time-series data. In Section 5, experimental research with the proposed method for a scaled jacket platform model under random load produced by a shaking table is presented, and the performance evaluation for different damage cases (including the combination of minor and major damage on different locations) is discussed. Finally, conclusions are drawn in Section 6.

2. Brief Introduction to the LSTM method

Traditional RNN can guarantee the continuity of information well and has achieved great success in text, image and speech identification. As shown in Fig. 1, x_t is the input information to neural network A, and the final output is h_t. It is seen that the information can be transferred from the current step to the next step in the RNN. However, if the transmission distance becomes longer, it is difficult to ensure the continuity of the information. In order to overcome this shortcoming, a LSTM network was proposed, which is a variant of RNN and has the ability to store long-distance historical information (Wu et al., 2018). As shown in Fig. 2, the configuration of the LSTM network has obvious differences with the RNN, consisting of three gates (the forget, input and output gates) and an update status.

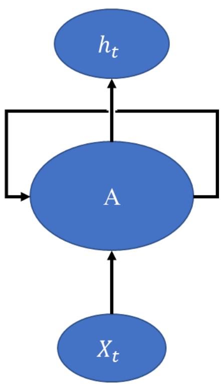

Fig. 1. Diagram of simple RNN.

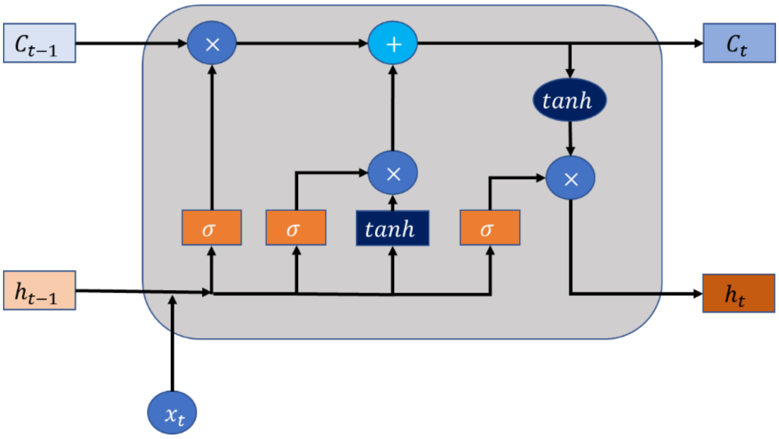

Fig. 2. Diagram of LSTM.

2.1 Forget gate

The forget gate is used to select which information needs to be discarded through the sigmoid layer. The diagram is shown in Fig. 3 (the red lines) and the output of the forget gate f_t can be expressed as

$$f_t = \sigma\left(W_f[h_{t-1}, x_t] + b_f\right) \tag{1}$$

where σ is the sigmoid function, h_{t-1} is the previous output, x_t is the current input, W_f is the weight, and b_f is the bias term. Note that the output of the forget gate should be converted into the value between 0 and 1 for the state of C_{t-1}, which represents the pass rate of the information. For example, 0 indicates that no information passes and 1 indicates that all information passes.

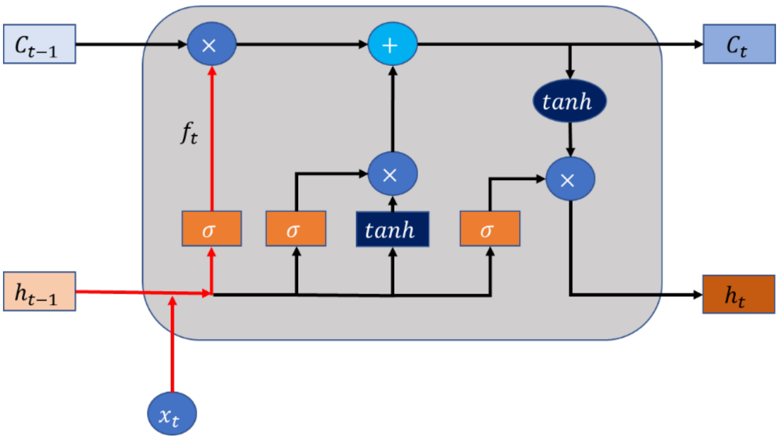

Fig. 3. Diagram of the forget gate (red lines).

2.2 Input gate

As shown in Fig. 4, the input gate serves to clarify the information that needs to be stored, which includes two parts: (i) obtaining the value that needs to be updated through the sigmoid layer and the update probability i_t that can be expressed as Eq. (2), and (ii) constructing the candidate vector $\widetilde{C}_t$ through the hyperbolic tangent function in Eq. (3):

$$i_t = \sigma(W_i[h_{t-1}, x_t] + b_i), \tag{2}$$

$$\widetilde{C}_t = \tanh\,(W_C[h_{t-1}, x_t] + b_c), \tag{3}$$

where W_i and W_C represent the weight, and b_i and b_c denote the bias term.

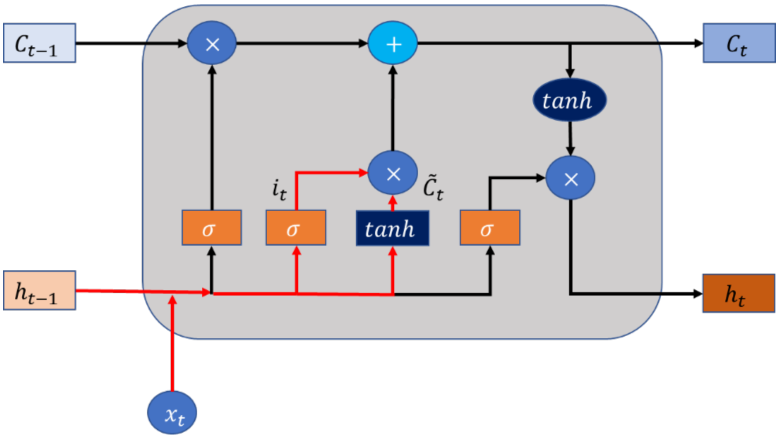

Fig. 4. Diagram of the input gate (red lines).

2.3 Update status

The update process from C_{t-1} to C_t (Fig. 5) is expressed by

$$C_t = f_t * C_{t-1} + i_t * \widetilde{C}_t, \tag{4}$$

where $*$ is the element-wise product. The element-wise product of C_{t-1} and f_t represents the information that needs to be forgotten, and the element-wise product of i_t and $\widetilde{C}_t$ represents the information that needs to be added.

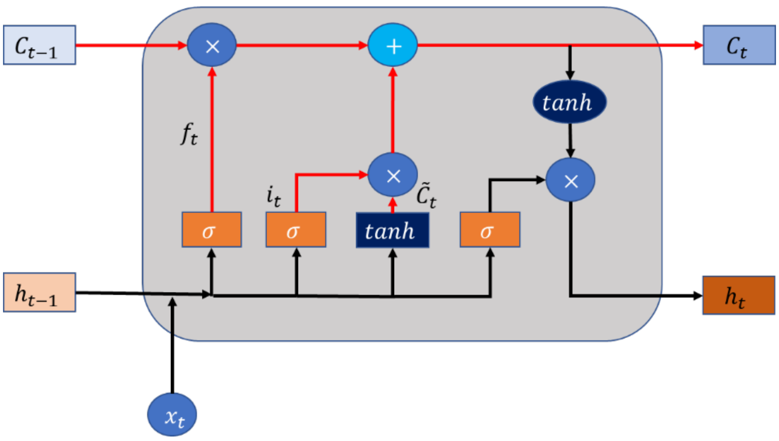

Fig. 5. Diagram of the update process (red lines).

2.4 Output gate

As shown in Fig. 6, the output gate serves to obtain the output information o_t through the sigmoid layer, and subsequently to obtain the final output h_t through the element-wise product of o_t and the processed information $\tanh(C_t)$ by the tanh function, which can be expressed as

$$o_t = \sigma(W_o[h_{t-1}, x_t] + b_o), \tag{5}$$

$$h_t = o_t * \tanh(C_t), \tag{6}$$

where W_o is the weight, and b_o is the bias term, and $*$ is the element-wise product.

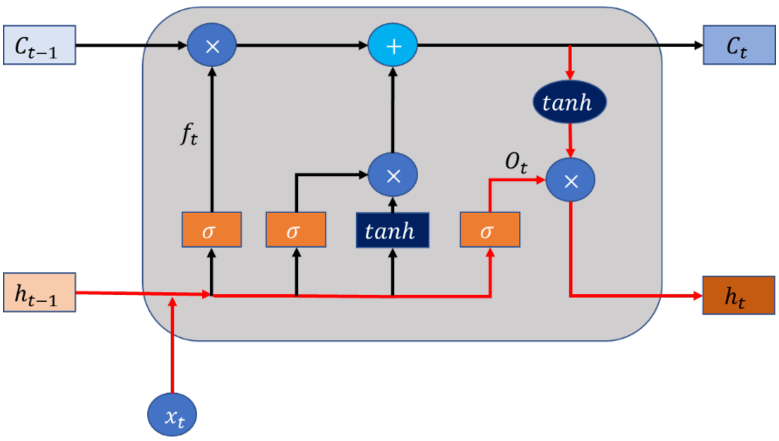

Fig. 6. Diagram of the output gate (red lines).

3. The concept of the random decrement technique

The RDT is a method of data processing, which refers to the conversion of random vibration response signals into free decaying vibration signals. The concept of the RDT is easy to understand and has been widely used to process the dynamic response data of large structures under environmental excitation for modal analysis or damage detection.

According to the derivation of Cole (1971), the random decrement function $\delta_{YY}(\tau)$ is regarded as the average of the time segments $y(t_i+\tau)$ of the response signal, and the triggering condition for each segment is $y(t_i)=a_0$, expressed as

$$\delta_{YY}(\tau)=\frac{1}{N}\sum_{i=1}^{N}\{y(t_i+\tau)|y(t_i)=a_0\}, \quad (7)$$

where $\tau=t-t_i$ is the time past the triggering time t_i, $and\ N$ represents the number of triggering points. Eq. (7) can be rewritten in a more general form,

$$\delta_{YY}(\tau)=E[y(t_i+\tau)|T_{y(t)}]. \quad (8)$$

The random decrement function $\delta_{YY}(\tau)$ is estimated as a conditional expected value. The value of the triggering condition ($T_{y(t)}$) is determined by the user, usually in the range of $(1\sim2)\sigma_y$, where σ_y is the standard deviation of the signal $y(t)$.

4. Numerical studies

4.1 Numerical model

A numerical model of a jacket platform was constructed using the ANSYS software. The dimensions of transverse brace (TB), pile leg (PL) and slanted brace (SB) of the model are illustrated in Table 1. The platform is about 60 m in height, located in a water depth of 41 m, and its superstructure weighs 2.8×10^5 kg. As described in Fig. 7, the superstructure of the platform is modeled as four lumped mass points placed on top of the four PLs. The material properties of the platform are as follows: density, 7850 kg/m^3; Poisson’s ratio, 0.3; and Young's modulus, 210 GPa. Assuming that the structure is excited by the random wave produced by ten regular waves with different wave heights (0.3-1.0 m) and periods (3.5-6.0 s) along the x direction in ANSYS, the damage simulation is to reduce the Young's modulus of one or more components of the structure.

Table 1 The dimensions of the jacket-type offshore platform

Component	External diameter (m)	Wall thickness (m)
Transverse brace (TB)	0.78	0.0381

Pile leg (PL)	1.2	0.05
Slanted brace (SB)	0.509	0.0254

4.2 Damage localization

It is a challenging work to identify minor damages of a complex structure. For evaluating the applicability of the proposed method, the damage severity simulated in this study is less than 5%. In this section, a total of 5 damage cases are analyzed, including 2 single and 1 multiple damage locations on whole segments, 1 single and 1 multiple damage locations on local elements (one-fifth of the whole segment) of PL, TB and SB, respectively. Altogether, 5 scenarios corresponding to each damage case are considered in this study, consisting of an intact and 4 damage scenarios. The details of the damage cases are clarified in Table 2 and Fig. 7 (a) to Fig. 7 (e). In case 5, for example, Fig. 7 (e) demonstrates the 4 multiple damage scenarios on local elements with different locations and different severities. For the first damage scenario, the damage severity is 5% for local element on TB, 2% for local element on PL, and 3% for local element on SB. The rest are similar to the first damage scenario.

The axial strain responses from 8 sampling points (channels) of the structure (Fig. 7 (f)) corresponding to the pre- and post-damage structure subjected to the random wave (Fig. 8 (a)) are obtained. Note that the 8 sampling channels are fixed for all the damage cases. Fig. 8 (b) describes the axial strain responses obtained from channel 1 corresponding to two scenarios (i.e., the intact and damage with 4% severity) in case 1. The difference between the time domain data in the two scenarios is found to be minor due to the minor damage severity.

Table 2. Damage cases of the numerical jacket-type offshore platform

Case	Damage location	Damage severity (%)
1	Whole segment of PL	2; 2; 3; 4
2	Whole segment of TB	2; 3; 4; 5
3	Whole segment of TB, PL, SB	5, 2, 3; 2, 3, 4; 3, 4, 5; 5, 5, 5
4	Local element of PL	2; 3; 4; 5
5	Local element of TB, PL, SB	5, 2, 3; 2, 3, 4; 3, 4, 5; 5, 5, 5

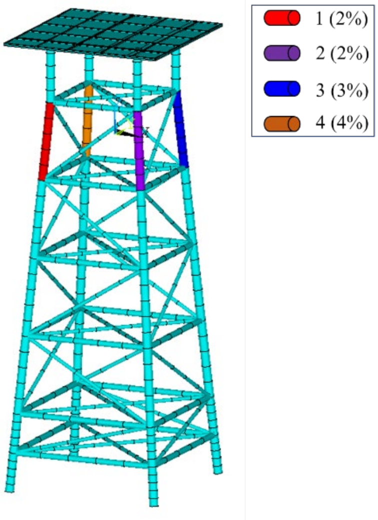

(a) case 1

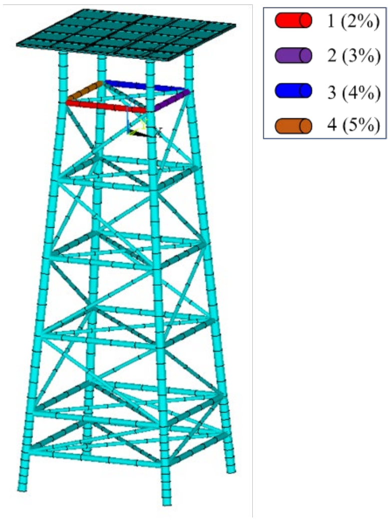

(b) case 2

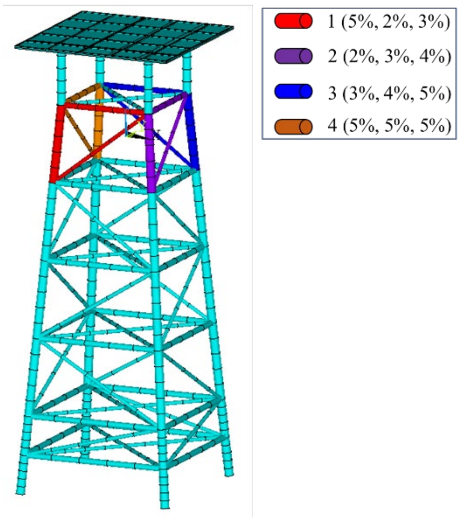

(c) case 3

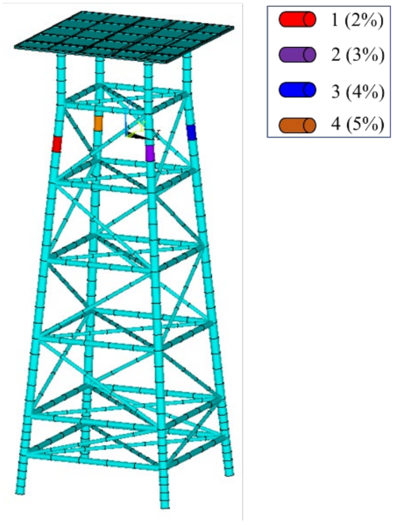

(d) case 4

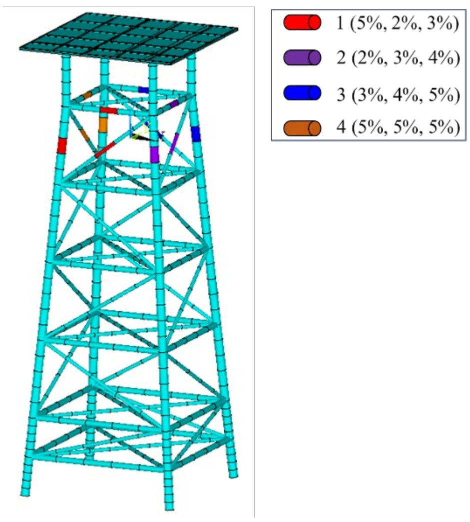

(e) case 5

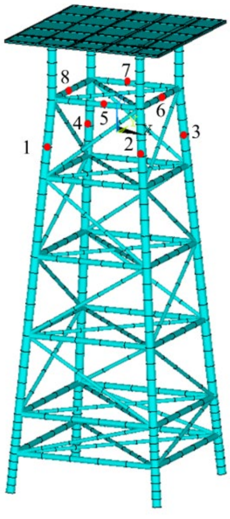

(f) sampling points

Fig. 7. Damage cases with different damage locations and severities and sampling points.

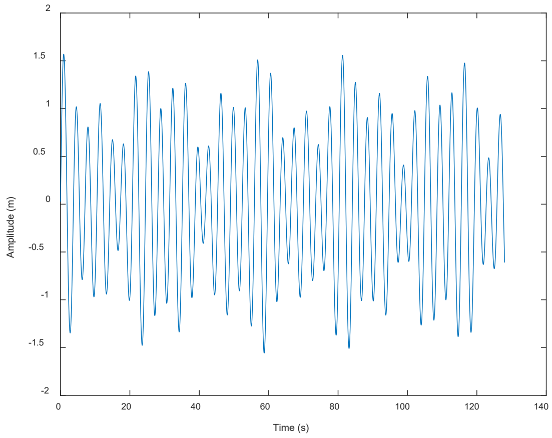

(a)

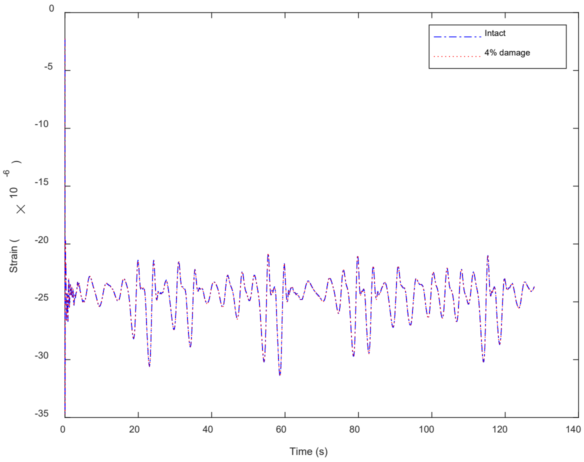

(b)

Fig. 8. The random wave (a) and strain responses obtained from channel 1 for 2 scenarios in case 1 (b).

4.2.1 Construction of LSTM network

The flowchart of LSTM network for damage detection in this work is described in Fig. 9. In order to improve the calculation efficiency, similar to the image recognition of a normal neural network, the one-dimensional vibration response data need to be transformed into two-dimensional time-series data, and then the standardization of the data is conducted by subtracting the original time-series data from the mean values and then dividing by its standard deviation. Thereafter, the standardized data are divided into the training dataset (70% of the data) and the testing dataset (30% of the data). During the training step, the LSTM networks are updated by determining the minimum value of the loss function. Note that the cross entropy function is selected to be the loss function in the damage localization process. Finally, in the testing or validation step the updated LSTM network is used to evaluate the prediction ability of damage localization based on the testing dataset.

The configuration of the LSTM network used in this work is as follows. The number of units is 120, the input shape is (10, 8) and the output shape is (1, 1). The Softmax function is utilized in the dense layer. Adam's algorithm is applied for the training process with a learning rate of 0.0001.

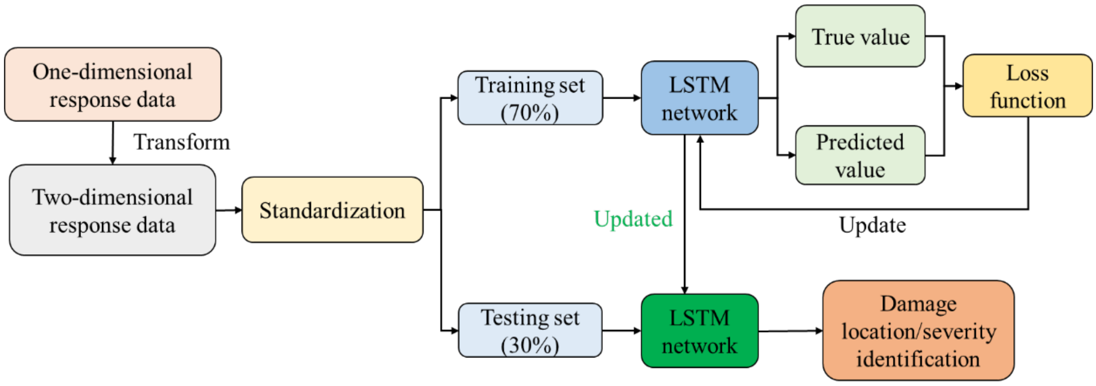

Fig. 9. The flowchart of LSTM network for damage localization and severity identification.

The length of the strain response data obtained from each of 8 points is 128 s with the sampling frequency 100 Hz. It follows that the size of the dataset corresponding to each scenario is 1280×10×8, and the total dimension of the dataset for the 5 scenarios of each damage case is 6400×10×8. The size of the training dataset is 4480×10×8 (70%), and the size of the testing dataset is 1920×10×8 (30%). It is noted that each datum should be labeled during the processing of LSTM. The intact scenario is labeled as 0 and the damage scenarios are labeled as 1, 2, 3, and 4, respectively, for all the 5 damage cases, which are clarified in Fig. 7 (a) to Fig. 7 (e).

Furthermore, the convergence history of training accuracy and loss value for damage case 1 is demonstrated in Fig. 10. It is seen that both the accuracy and loss value reach a stable state after 300 iterations. The calculation time of damage case 1 for the epoch of 300 is 296.8 s, with a computer configuration consisting of an Intel core i7-9750H CPU, the Windows 64-bit V10 system and Python 3.7.

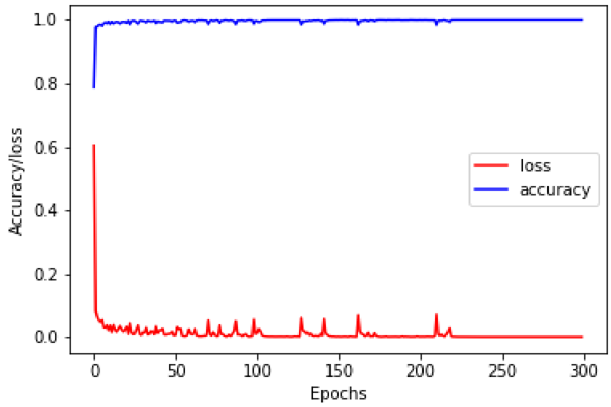

Fig. 10. Convergence history of training accuracy and loss value for damage case 1.

4.2.2 Damage localization Results

The results of damage localization for each of the 5 damage cases is described by the confusion matrix (see Fig. 11 (a) to (e)), in which the prediction accuracy of the LSTM for different damage locations with different damage severities is illustrated, respectively. The confusion matrix is usually applied to evaluate the quality of the output of a classifier. In this study, the diagonal elements represent the probabilities of the predicted label being equal to the true label, whereas the off-diagonal elements represent the probabilities of mislabeling by the classifier. The higher the trace of the confusion matrix (i.e., the sum of the elements on its main diagonal), the better, indicating many correct predictions. The sum of the elements in each row is 100%.

For example, the damage case 1 (single damage location on whole segment of PL), Fig. 11 (a), shows that the damage localization accuracy of label 0 (intact scenario) is 95.92%, while the probability of misidentifying label 0 as label 1 is 3.53%, and the probability of misidentifying label 0 as label 2 is 0.55%. Similarly, the damage localization accuracy of label 1 is 92.7%, label 2 is 100%, label 3 is 98.45%, and label 4 is 99.75%. The mean identification accuracy for damage case 1 is then calculated to be 97.37% from the 5 diagonal elements.

Fig. 11 (b) and (c) demonstrate the prediction accuracies of the LSTM for damage cases 2 (single damage location on whole segment of TB) and 3 (multiple damage locations on whole segments of TB, PL, SB), respectively. The mean prediction accuracies can be calculated to be 98.79 % for case 2 and 99.43% for case 3.

Furthermore, Fig. 11 (d) and (e) demonstrate the prediction accuracies of the LSTM for damage cases 4 (single damage location on local element of PL) and 5 (multiple damage locations on local elements of TB, PL, SB), respectively. It is calculated that the mean prediction accuracies are 98.27 % and 99.37% for case 4 and case 5, respectively.

The results show that LSTM is capable of determining damage locations for the jacket platform with great accuracy, both for the whole segments or the local elements, even though the damage severity is very small. Furthermore, the prediction accuracies are slightly higher for the multiple damage locations than those for the single damage location.

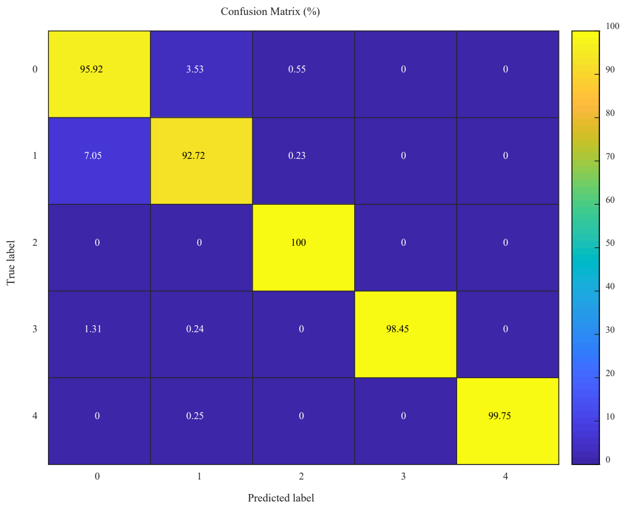

(a) case 1

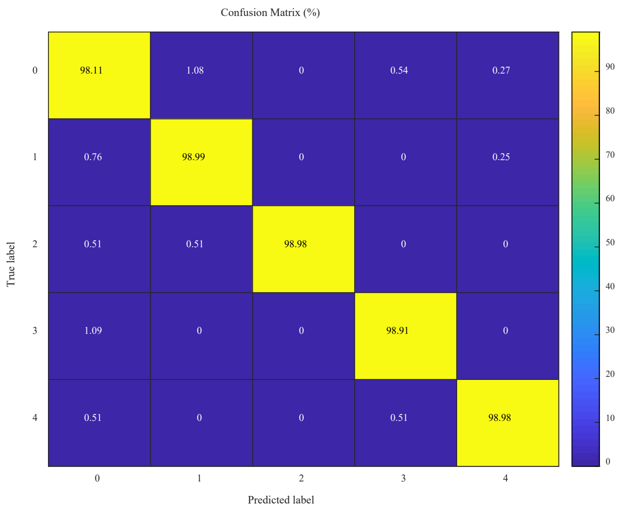

(b) case 2

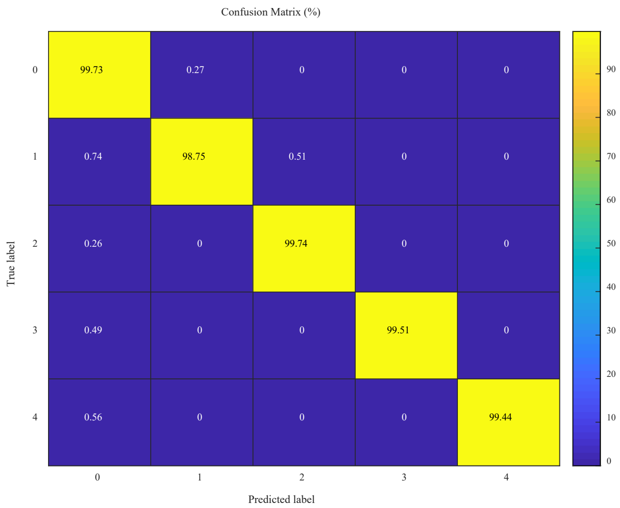

(c) case 3

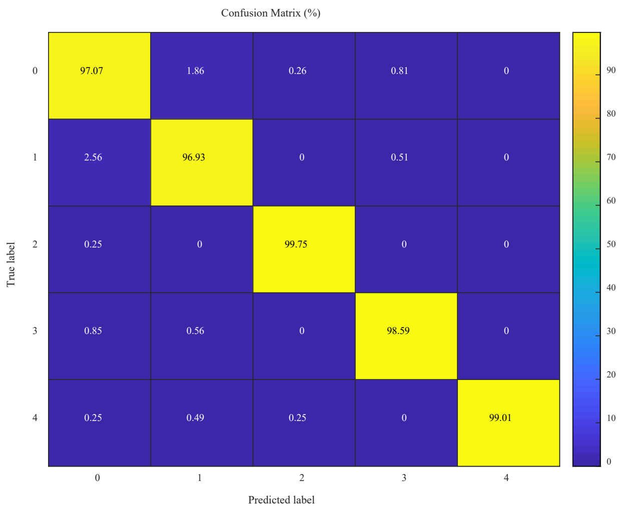

(d) case 4

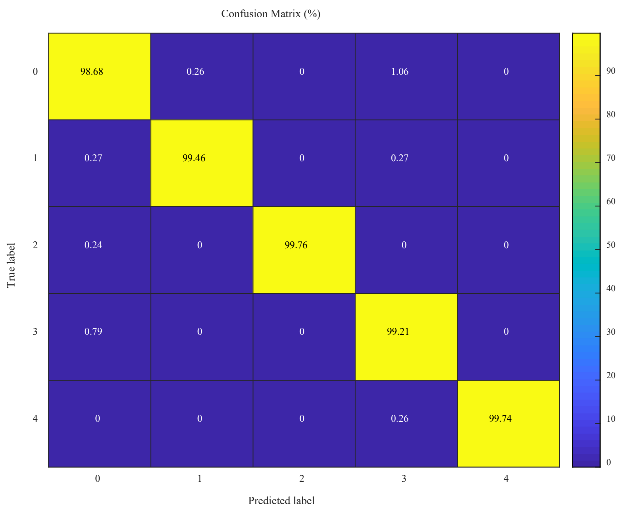

(e) case 5

Fig. 11. Confusion matrix of the damage localization for 5 cases, respectively.

4.3 Damage localization considering the influence of noise

In real engineering, it is inevitable that the measured vibration response data will be contaminated by noise. At the same time, for proving the effectiveness of the RDT and LSTM method under the noise condition, additive Gaussian white noise is considered with 5%, 10%, and 20% noise level.

Without loss of generality, the damage case 5 with several noise levels is considered in this section. In addition, the traditional machine learning method SVM is applied to identify the damage location for comparison with the LSTM. The method of parameter optimization is used to find the best parameters of SVM as $C = 1, \gamma = 0.092$, and kernel='rbf'. The results of identification accuracy for case 5 with several noise levels are listed in Table 3. It is seen that both the LSTM and SVM methods can identify the damage location with accuracy more than 99% based on the noise free data. However, with the increase in noise level, the accuracy of the two methods decreases significantly, most notably in the case of the SVM method.

Table 3 The damage localization accuracy of case 5 with different noise levels (%)

Method	Noise level (%)			
	0	5	10	20
LSTM	99.4	71.5	51.3	32.7
SVM	99.3	41.7	30.4	24.4
RDT+LSTM	100	100	100	100
RDT+SVM	100	100	100	100

For overcoming the influence of noise on the LSTM method, the RDT is applied for noisy data preprocessing (Fig. 12). For the noisy data of each channel of each damage case, the length of output data is set to 6400 (i.e., half length of the noisy data) and the triggering condition is selected to be 1.2 times the standard deviation of the noisy signal during the RDT process. Then the new (processed) data are obtained by averaging the subsamples of the noisy signal. After the signal processing based on RDT for the noisy data of the 5 damage cases, the dimension of the new dataset becomes 50% of the original dataset. Then the LSTM and SVM methods are applied to identify the damage location. Table 3 also lists the results of identification accuracy using LSTM and SVM after data preprocessed by RDT for damage case 5 with different noise levels. It is found that the damage localization accuracy of the two methods combined with RDT has been significantly improved, reaching 100% even for the 20% noise level.

Fig. 13 (a), (b) and (c) show the original data, noisy data with 20% noise level and processed data by RDT of channel 1 with 5 scenarios (labels) in damage case 5, respectively, which can be the possible explanations for the differences between the damage localization accuracy based on the original data, noisy data and processed data. In Fig. 13 (a) the differences of the original data among the 5 labels are less visible, since the damage severities at different positions are small. However, the identification accuracies are still more than 99% using both the LSTM and SVM methods. It is worth noting that the noisy data corresponding to the 5 labels (Fig. 13 (b)) are extremely confused and not easy to distinguish by LSTM or SVM alone. Furthermore, the data processed by RDT are shown in Fig. 13 (c), from which we can find the obvious differences between the intact (label 0) and damage scenarios (label 1, 2, 3 and 4), even though the differences among the damage scenarios are still not very visible. The results indicate that the proposed RDT-LSTM approach is capable of localizing the damage from the noisy data with great accuracy even if the damage severity is very small.

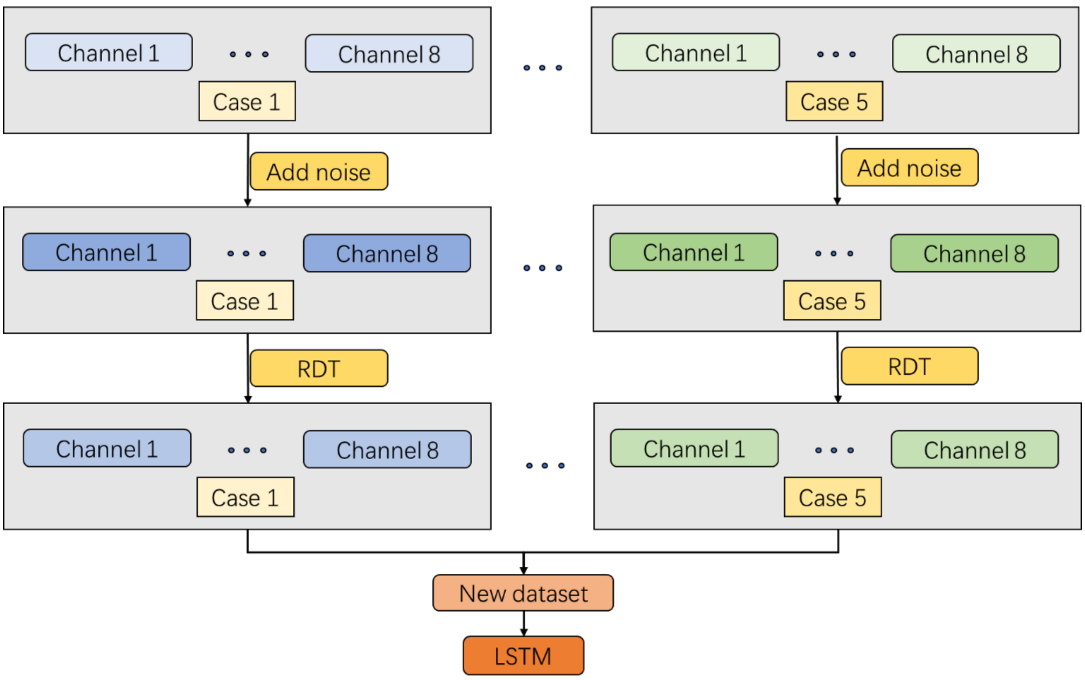

Fig. 12. Flowchart of noisy data preprocessing by RDT

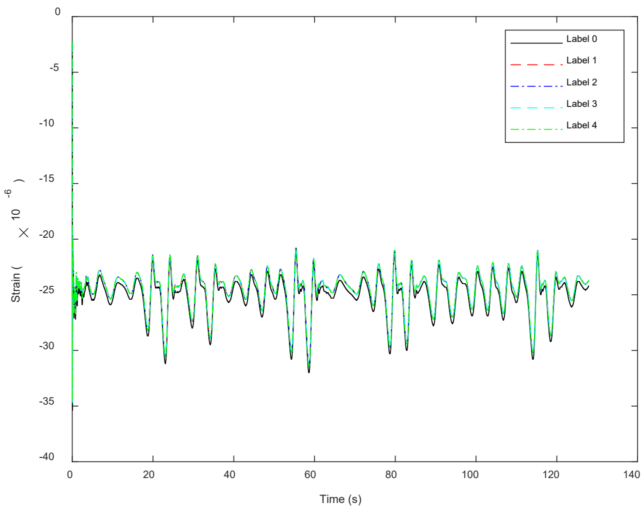

(a) original data

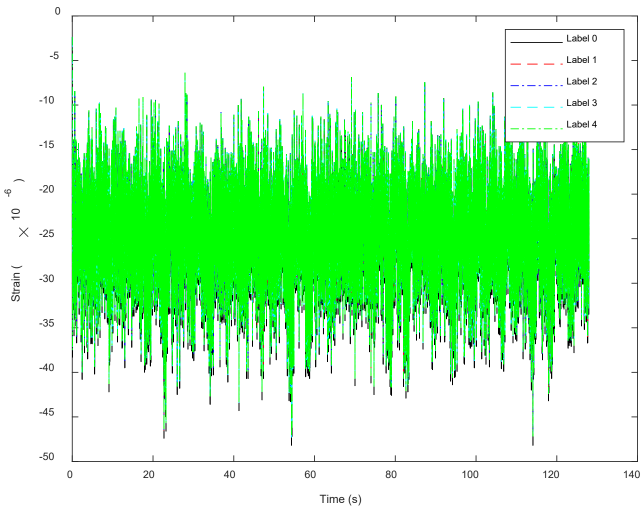

(b) noisy data with 20% noise level

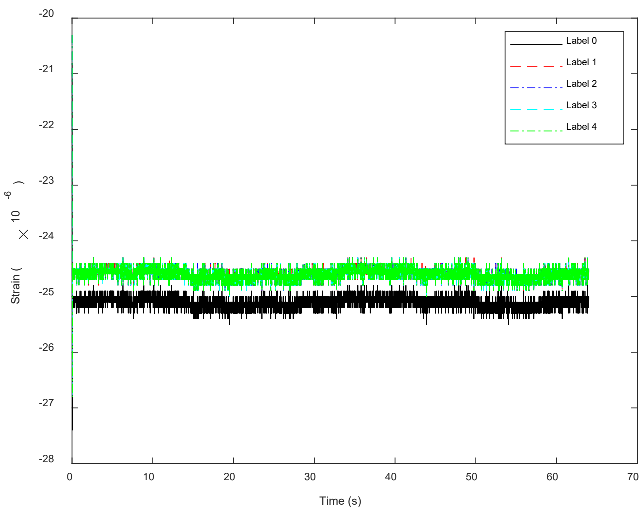

(c) processed data by RDT

Fig. 13. Original, noisy and processed data from channel 1 with 5 scenarios of damage case 5.

4.4. Identification of the damage severity

As the LSTM method has been validated in the simulation to be able to accurately identify and localize the damage on no matter whole segments or local elements, the verification of the effectiveness of the LSTM method for minor and close damage severity identification is then carried out in this section for local elements of the structure (see Fig. 14) subjected to random wave excitation in y-direction. The minor damage severity on different locations is randomly generated between 1% and 5%.

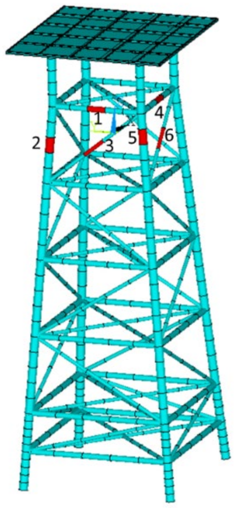

Fig. 14. The simulated damage locations for damage severity identification.

The LSTM adopts the regression method to identify the damage severity and the mean square error to be the loss function. The performances of the LSTM method for damage severity identification are demonstrated based on the original data, noisy data with 5% noise level, and processed data by the RDT, respectively. Table 4 lists the damage severity estimation results for 4 damage cases, including 2 single-damage cases, and 2 multiple-damage cases. It is seen that the estimation error based on the original data is very little, no more than 2.00%, while based on the noisy data the maximum error is 33.33%. However, the accuracy of the damage severity identification based on the processed data by RDT for noisy data is quite high, with error no more than 1.50%.

The results indicate the LSTM method can effectively estimate the minor and close damage severity of the local element of a structure based on the clean vibration response data. In the case of noisy data, however, the identification accuracy of the damage severity can be significantly improved by the proposed RDT-LSTM method.

Table 4 The damage severity identification for single and multiple local elements based on original data, noisy data and processed data.

Case	1	2	3			4		
Damage location	1	6	1	2	3	4	5	6
Actual severity (%)	4.00	3.00	2.00	3.00	4.00	5.00	2.00	3.00
Identification with original data (%)	3.92	2.96	1.99	2.98	3.97	5.00	2.02	3.02
Error (%)	2.00	1.33	0.50	0.67	0.75	0	1.00	0.67
Identification with noisy data (%)	4.99	2.00	1.90	2.55	3.36	4.15	2.42	3.36
Error (%)	24.75	33.33	5.00	15.00	16.00	17.00	21.00	12.00
Identification with data preprocessing (%)	3.96	2.96	2.03	3.03	4.04	5.02	2.00	3.01
Error (%)	1.00	1.33	1.50	1.00	1.00	0.40	0	0.33

Nevertheless, for the sake of comparison with LSTM, the traditional machine learning method SVM has also been applied to identify the damage severity. The results of identification for 4 single-damage cases without consideration of the noise are listed in Table 5. It is found that the errors of the damage severity identification in different cases with SVM are much larger than those with LSTM, especially in cases with very minor damage case (e.g., case 5). Based on these results, the SVM and RDT-SVM methods for the damage severity identification under noise conditions are not used in this work.

Traditional machine learning methods present obvious limitations compared with deep learning methods (Abdeljaber et al., 2017; Lin et al., 2018). SVM, for example, has inherent shortcomings – its noise resistance is poor, and its process of parameter optimization is computationally expensive.

Table 5 Comparison of the LSTM and SVM for damage severity identification.

Method	Case	5	6	7	8
	Damage location	1	2	4	6
	Actual severity (%)	2.00	3.00	4.00	5.00
SVM	Identification (%)	1.64	2.74	3.69	4.58
	Error (%)	18.0	8.67	7.75	8.40
LSTM	Identification (%)	1.97	2.96	3.92	4.99
	Error (%)	1.50	1.33	2.00	0.20

5. Experimental study

The experimental study of the proposed RDT-LSTM approach for damage detection was also conducted for a steel jacket platform model under the random load produced by a shaking table. As shown in Fig. 15, the jacket platform model was placed in a sand bucket, and the bucket was fixed with bolts onto the shaking table. The layer spacing of the model is 15 cm, 15 cm, 25 cm, 30 cm and 30 cm, respectively. The outer diameter and thickness of the pile legs is 20 mm×2 mm, and those of the transverse braces and slanted braces are 12 mm×2 mm. The dimensions of the two decks are 460 mm×460 mm×6 mm. The inclinations of the 4 pile legs are 1:10.

As shown in Fig. 16, there were 20 strain gauges mounted on the members of the structure with the connection of half-bridge; that is, 10 channels were constructed to acquire the vibration response data in the experiment using the dynamic data acquisition system. The damage was simulated through removing some of the bolts on a segment of the member. Note that there are 8 bolts in both sides of the small segment, i.e., 4 bolts in each side. Two kinds of damage severity were tested in this experiment, including the major and minor damage on the members of TB, PL, and SB. The major damage was produced by removing all the 8 bolts on the member and then completely detaching the small segment. While the minor damage was produced by removing only 4 bolts on one side of the segment and by imposing that the segment remain in contact with the member (see Fig. 15). A total of 8 damage cases were simulated in the experiments, including the major and minor damages on different members and their combination. Table 6 lists the damage locations, severities and labels needed in the processing of LSTM.

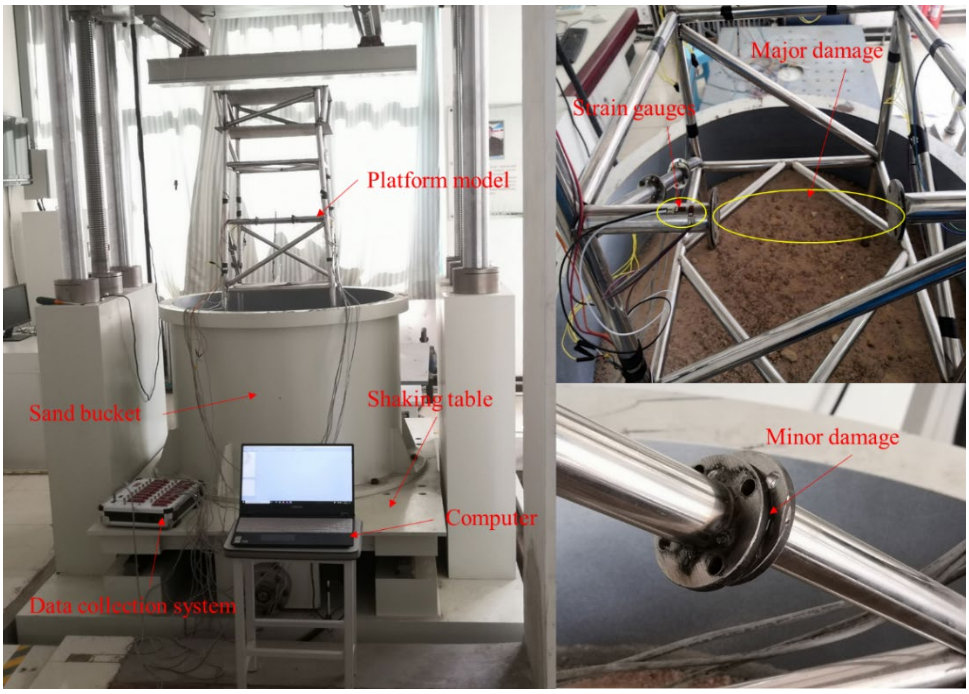

Fig. 15. The experimental model of the jacket-type offshore platform.

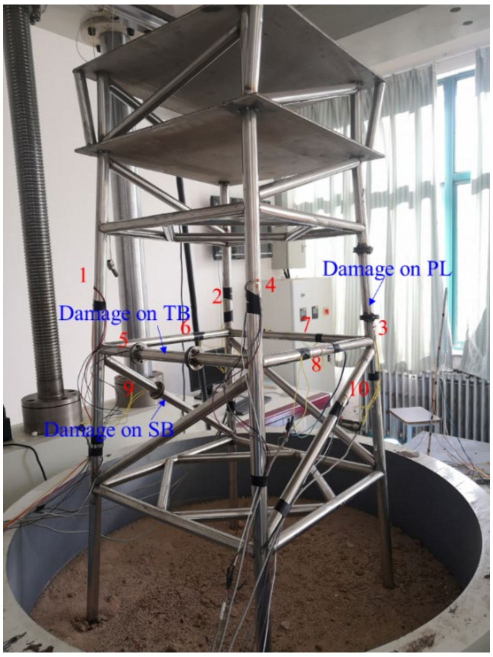

Fig. 16. The placement of the strain gauges and damage locations.

Table 6 Damage cases of the jacket-type offshore platform model.

Case	Location	Label
1	intact	0
2	minor damage on TB	1
3	minor damage on TB and SB	2
4	minor damage on TB, SB and PL	3
5	minor damage on TB and PL	4
6	major damage on SB	5
7	major damage on TB and PL and minor damage on SB	6
8	major damage on TB, SB and PL	7

In each of the 8 damage cases, the dynamic data acquisition system was used to collect the strain response data from 10 channels under the random excitation. The sampling frequency was 1024 Hz and sampling time 60 s. Fig. 17 illustrates a 12.5 s segment of strain response signals acquired from channel 1 corresponding to the 8 damage cases, respectively. It is found that there are some differences among the amplitudes of the data in the different cases, as expected, but the differences corresponding to some cases (labels) are not very significant, for example labels 1 and 5, labels 3 and 7.

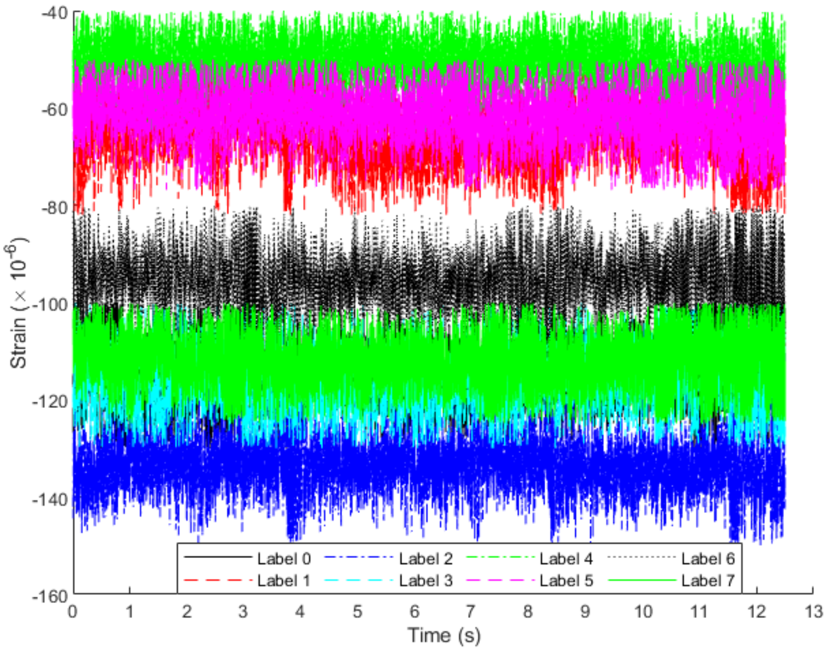

Fig. 17. The data collected from channel 1 corresponding to 8 damage cases.

The total dataset constructed with the dimension of 10240×10×10 was input into the LSTM for damage localization. 70% of the data, with the size of 7168×10×10, were used as the training dataset, and 30% of the data, with the size of 3072×10×10, were used as the testing dataset. As illustrated in Fig. 18, the performance of the LSTM for determining the damage locations of the jacket platform model is satisfactory, with the prediction accuracy of more than 99% and 100% for 5 of the 8 cases.

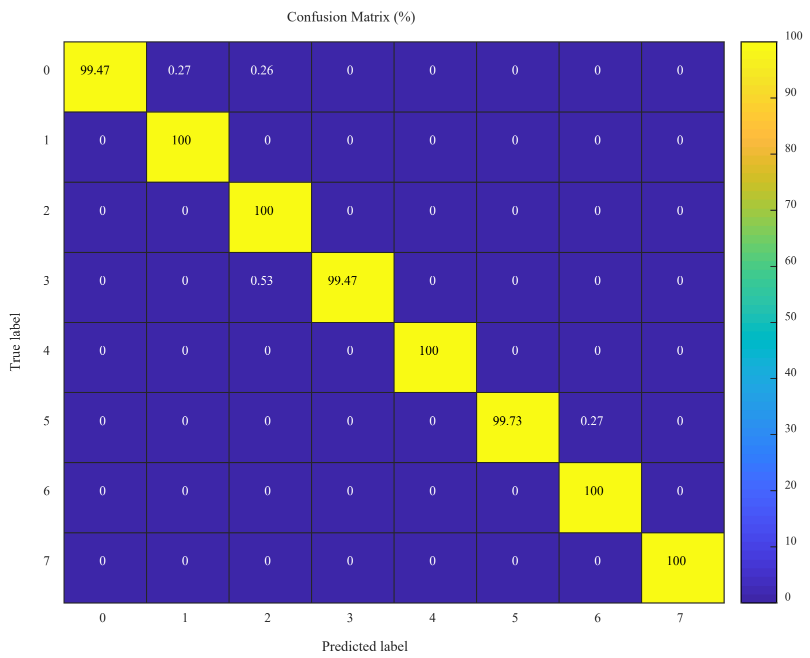

Fig. 18. Damage identification accuracy of different cases using LSTM.

Although the noise level in the experiment maybe small, the effectiveness of the RDT-LSTM method was also studied in this section in order to provide references for its application in engineering. The RDT was first used for the collected data from each channel corresponding to each damage case to reconstruct the dataset. As shown in Fig. 19, the length of the processed data by the RDT was one-half of the original data. In addition, the amplitude differences of the processed data among different damage cases were much more significant than those of the original data (Fig. 17). Then the LSTM was applied to identify and localize the damages based on the processed data. As shown in Fig. 20, the prediction accuracy is 100% for all the 8 damage cases. The result demonstrates that the performance of the RDT-LSTM method for damage localization is outstanding, even though the damage cases are complicated, including major and minor damages on different members and their combination.

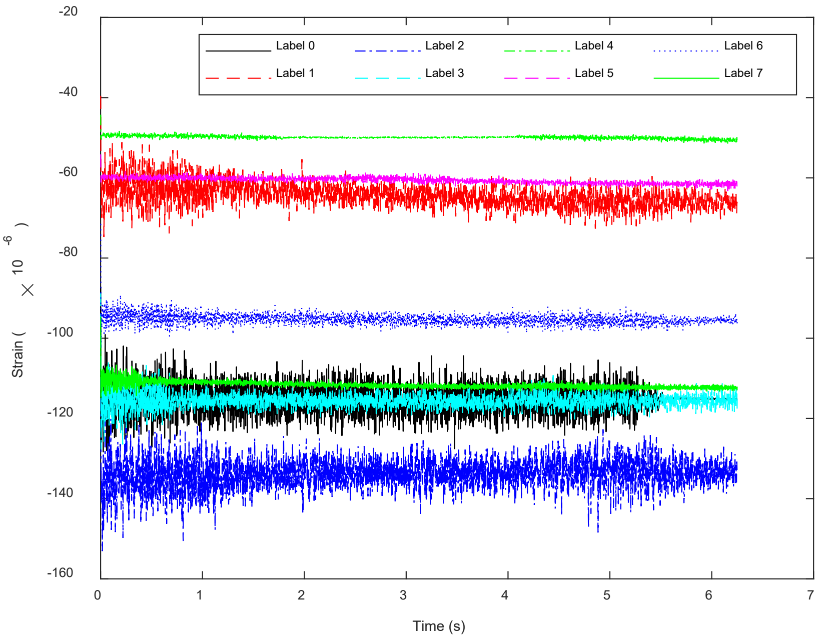

Fig. 19. The processed data by RDT from channel 1 corresponding to 8 damage cases.

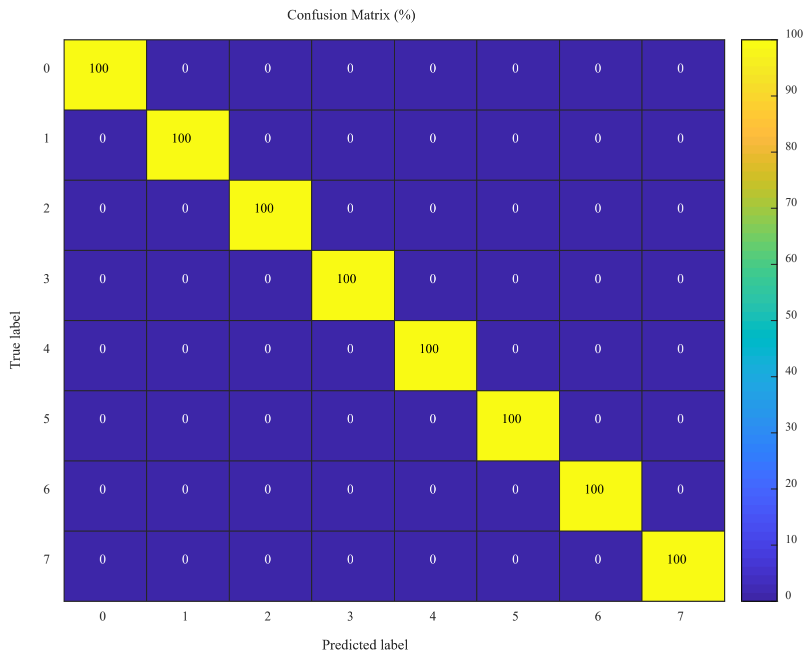

	0	1	2	3	4	5	6	7
0	100	0	0	0	0	0	0	0
1	0	100	0	0	0	0	0	0
2	0	0	100	0	0	0	0	0
3	0	0	0	100	0	0	0	0
4	0	0	0	0	100	0	0	0
5	0	0	0	0	0	100	0	0
6	0	0	0	0	0	0	100	0
7	0	0	0	0	0	0	0	100

Fig. 20. Damage identification accuracy of different cases using RDT-LSTM.

6. Conclusions

The RDT-LSTM method is proposed in this study for the localization and severity assessment of random vibration-based structural damage, especially in noisy conditions. The RDT is first applied to preprocess the collected random vibrational response data. Then, the LSTM for damage detection is conducted on the basis of the processed time series data. The RDT-LSTM method is validated by means of a numerical application and laboratory tests of jacket platforms subjected to a random excitation. The main conclusions are as follows.

First, in the absence of noise, the LSTM approach has an excellent performance in determining the presence, location and severity of single and multiple damage, even when the simulated damage severities are very small (no more than 5%) and on local elements (one-fifth of the whole segment) of the numerical structure. With increasing noise levels, the accuracy of damage localization and severity identification of the LSTM method reduces significantly.

Second, the utilization of the RDT for random vibration response data preprocessing can remarkably improve the capability of damage localization and severity identification of the LSTM method in noisy conditions.

Third, the experimental research results show that the RDT-LSTM approach can accurately identify and localize the damage of the jacket platform model under random excitation, including the minor and major damages on different members and their combination.

In summary, these results indicate that the RDT-LSTM method combined with certain types of vibration measurement and signal transmission system constitutes a practical and effective approach to the SHM of offshore structures.

Acknowledgments

This research is supported by the National Natural Science Foundation of China (Grant No. 51979283), the Shandong Provincial Natural Science Foundation, China (Grant No. ZR2018MEE053), the Fundamental Research Funds for the Central Universities (Grant No. 20CX02313A) and the Opening Fund of National Engineering Laboratory of Offshore Geophysical and Exploration Equipment (Grant No. 20CX02313A). G. Iglesias is grateful for the support of Science Foundation Ireland (SFI) and MaREI, the Marine Renewable Energy Centre Ireland, grant SFI MAREI2_12/RC/2302/P2

Platform RA1b.

References

Abdeljaber, O., Avci, O., Kiranyaz, S., et al., 2017. Real-time vibration-based structural damage detection using one-dimensional convolutional neural networks. J. Sound Vib. 388, 154-170.

Abdeljaber, O., Avci, O., Kiranyaz, S., et al., 2018. 1-D CNNs for structural damage detection: verification on a structural health monitoring benchmark data, Neurocomputing. 275, 1308-1317.

Alom, M.Z., Taha, T.M., Yakopcic, C., et al., 2019. A state-of-the-art survey on deep learning theory and architectures. Electronics 8, 292.

Amezquita-Sanchez, J.P., Adeli, H., 2016. Signal processing techniques for vibration-based health monitoring of smart structures. Arch. Comp. Meth. Eng. 23(1), 1-15.

Asgarian, B., Aghaeidoost, V., Shokrgozar, H.R., 2016. Damage detection of jacket type offshore platforms using rate of signal energy using wavelet packet transform. Mar. Struct. 45, 1-21.

Ashory, M.R., Ghasemi-Ghalebahman, A., Kokabi, M.J., 2017. An efficient modal strain energy-based damage detection for laminated composite plates. Adv. Compos. Mater. 27(2), 147-162.

Avci, O., Abdeljaber, O., Kiranyaz, S., et al., 2018. Wireless and real-time structural damage detection: A novel decentralized method for wireless sensor networks. J. Sound Vib. 424, 158-172.

Avci, O., Abdeljaber, O., Kiranyaz, S., et al., 2021. A review of vibration-based damage detection in civil structures: From traditional methods to Machine Learning and Deep Learning applications. Mech. Syst. Signal Pr. 147, 107077.

Bandara, R.P., Chan, T.H.T., Thambiratnam, D.P., 2013. The three-stage artificial neural network method for damage assessment of building structures. Aust. J. Struct. Eng. 14, 13-25.

Bandara, R.P., Chan, T.H.T., Thambiratnam, D.P., 2014. Structural damage detection method using frequency response functions. Struct. Heal. Monit. 13, 418-429.

Bao, T., Swartz, R. A., Vitton, S., et al., 2017. Critical insights for advanced bridge scour detection using the natural frequency. J. Sound Vib. 386, 116-133.

Bao, X.X., Fan, T.X., Shi, C., et al., 2021. One-dimensional convolutional neural network for damage detection of jacket-type offshore platforms. Ocean Eng. 219, 108293.

Bao, X.X., Sun, H.H., Iglesias, G., et al., 2020. Signal denoising method for modal analysis of an offshore platform. J. Loss Prevent. Proc. 63, 104000.

Bao, X.X., and Shi, C., 2019. Ambient vibration responses denoising for operational modal analysis of a jacket-type offshore platform. Ocean Eng. 172, 9-21.

Brincker, R., Ventura, C., 2015. Introduction to Operational Modal Analysis. John Wiley & Sons.

Budipriyanto A., Haddara M.R., Swamidas A.S.J., 2007. Identification of damage on ship's cross-stiffened plate panels using vibration response. Ocean Eng. 34(5–6), 709-716.

Cole H.A. On the line analysis of random vibration. Proceedings of the AIAA/ASME 9th Structures, Structural Dynamics and Materials Conference, Palm Springs, California; 1968.

Cole, H.A. Failure detection of a space shuttle wing by random decrement. Technical Report NASA TMX-62041, 1971.

Dackermann, U., Li, J., Samali, B., 2010. Dynamic-based damage identification using neural network ensembles and damage index method. Adv. Struct. Eng. 13, 1001-1016.

Dehcheshmeh, M.M., Hosseinzadeh, A.Z., Amiri, G.G., 2020. Feasibility study on model-based damage detection in shear frames using pseudo modal strain energy. Smart Struct. Syst. 25(1), 47-56.

Ding, Z.H., Huang, M., Lu, Z.R., 2016. Structural damage detection using artificial bee colony algorithm with hybrid search strategy. Swarm Evol. Comput. 28, 1-13.

Elshafey, A.A., Haddara, M.R., Marzouk, H., 2010. Damage detection in offshore structures using neural networks. Mar. Struct. 23, 131-145.

Ercolani, G.D., Felix, D.H., Ortega, N.F., 2018. Crack detection in prestressed concrete structures by measuring their natural frequencies. J. Civ. Struct. Health Monit. 8(4), 661-671.

Feng, Z.Q., Shen, W.N., Chen, Z.Q., 2017. Consistent multilevel RDT-ERA for output-only ambient modal identification of structures. Int. J. Struct. Stab. Dy. 17(09), 1750106.

Figueiredo, E., Park, G., Farrar, C.R., et al., 2011. Machine learning algorithms for damage detection under operational and environmental variability. Struct. Heal. Monit. 10, 559-572.

Gui, G., Pan, H., Lin, Z., et al., 2017. Data-driven support vector machine with optimization techniques for structural health monitoring and damage detection. KSCE J. Civ. Eng. 21, 523-534.

Haeri, M.H, Lotfi, A, Dolatshahi, K.M., et al., 2017. Inverse vibration technique for structural health monitoring of offshore jacket platforms. Appl. Ocean Res. 62, 181-198.

Hu, S.-L.J., Yang, W.L., and Li, H.J., 2013. Signal decomposition and reconstruction using complex exponential models. Mech. Syst. Signal Pr. 40, 421-438.

Ince, T., Kiranyaz, S., Eren, L., et al., 2016. Real-time motor fault detection by 1-D convolutional neural networks. IEEE. T. Ind. Electron. 63, 7067-7075.

Jahangiri, V., Mirab, H., Fathi, R., et al., 2016. TLP structural health monitoring based on vibration signal of energy harvesting system. Lat. Am. J. Solids Struct. 13(5), 897-915.

Khodabandehlou, H., Pekcan, G., Fadali, M.S., 2019. Vibration-based structural condition assessment using convolution neural networks. Struct. Contr. Health Monit. 2, e2308.

Kiranyaz, S., Gastli, A., Ben-Brahim, L., et al., 2018. Real-time fault detection and identification for MMC using 1D convolutional neural networks. IEEE Trans. Ind. Electron. 66, 8760-8771.

Li, H.J., Wang, J.R., Hu, S.L.J., 2008. Using incomplete modal data for damage detection in offshore jacket structures. Ocean Eng. 35(17-18), 1793-1799.

Li, Y.C., Wang, S.H., Zhang, M., et al, 2016. An improved modal strain energy method for damage detection in offshore platform structures. J. Mar. Sci. Appl. 15(2), 182-192.

Lin, C.S., Chiang, D.Y., 2012. A modified random decrement technique for modal identification from nonstationary ambient response data only. J. Mech. Sci. Technol. 26(6), 1687-1696.

Lin, R.M., Ng, T.Y., 2018. Applications of higher-order frequency response functions to the detection and damage assessment of general structural systems with breathing cracks. Int. J. Mech. Sci. 148, 652-666.

Lin, Z., Pan, H., Gui, G., et al., 2018. Data-driven structural diagnosis and conditional assessment: from shallow to deep learning. Conference: Sensors and Smart Structures Technologies for Civil, Mechanical, and Aerospace Systems, March 2018.

Liu, F.S., Fu, Q., and Tian, Z., 2019(a). A Laplace-domain method for motion response estimation of floating structures based on a combination of generalised transfer function and partial fraction. Ships Offshore Struct. 15, 829-843.

Liu, F.S., Gao, S.J., Han, H.W., Tian, Z., and Liu, P., 2019(b). Interference reduction of high-energy noise for modal parameter identification of offshore wind turbines based on iterative signal extraction. Ocean Eng. 183, 372-383.

Liu, F.S., Gao, S.J., Tian, Z., and Liu, D.Z., 2020. A new time-frequency analysis method based on single mode function decomposition for offshore wind turbines. Mar. Struct. 72, 102782.

Liu, F.S., Li, H.J., Li, W., et al., 2014. Experiment study of improved modal strain energy method for damage localization in jacket-type offshore wind turbines. Renew. Energ. 72, 174-181.

Liu, H., Zhang, Y., 2019. Image-driven structural steel damage condition assessment method using deep learning algorithm. Measurement 133, 168-181.

Luo, H., Huang, M.H., Zhou, Z., 2019. A dual-tree complex wavelet enhanced convolutional LSTM neural network for structural health monitoring of automotive suspension. Measurement 137, 14-27.

Mao, H.L., Tang, W.L., Huang, Y., et al., 2018. The construction and comparison of damage detection index based on the nonlinear output frequency response function and experimental analysis. J. Sound Vib. 427, 82-94.

Mohan, S.C., Maiti, D.K., Maity, D., 2013. Structural damage assessment using FRF employing particle swarm optimization. Appl. Math. Comput. 219(20), 10387-10400.

Morsy, R., Marzouk, H., Haddara, M., et al., 2017. Multi-channel random decrement smart sensing system for concrete bridge girders damage location identification. Eng. Struct. 143, 469-476.

Nichols, J.M., 2003. Structural health monitoring of offshore structures using ambient excitation. Appl. Ocean Res. 25(3), 101-114.

Ren, L., Li, H., Zhou, J., et al., 2006. Health monitoring system for offshore platform with fiber Bragg grating sensors. Opt. Eng. 45(8), 084401.

Santos, A., Figueiredo, E., Silva, M.F.M., et al., 2016. Machine learning algorithms for damage detection: Kernel-based approaches. J. Sound Vib. 363, 584-599.

Shiryayev, O.V., Slater, J.C., 2008. Improved structural damage identification using random decrement signatures: Application to FEM data. Struct. Control Health Monit. 15, 1006-1020.

Sony, S., Dunphy, K., Sadhu, A., et al., 2021. A systematic review of convolutional neural network-based structural condition assessment techniques. Eng. Struct. 226, 111347.

Tan, Z.X., Thambiratnam, D.P., Chan, T.H.T., et al., 2017. Detecting damage in steel beams using modal strain energy based damage index and Artificial Neural Network. Eng. Fail. Anal. 79, 253-262.

Truong, T.T, Dinh-Cong, D., Lee, J., et al., 2020. An effective deep feedforward neural networks (DFNN) method for damage identification of truss structures using noisy incomplete modal data. J. Build. Eng. 30, 101244.

Wang, S.Q., Xu, M.Q., 2019. Modal strain energy-based structural damage identification: a review and comparative study. Struct. Eng. Int. 29(2), 234-248.

Wang, S.Q., Xu, M.Q., Xia Z.P., and Li, Y.C., 2019. A novel Tikhonov regularization-based iterative method for structural damage identification of offshore platforms. J. Mar. Sci. Tech. 24, 575-592.

Wu, Y.T., Yuan, M., Dong, S.P., et al., 2018. Remaining useful life estimation of engineered systems using vanilla LSTM neural networks. Neurocomputing 275, 167-179.

Xu, Y., Wei, S., Bao, Y., et al., 2019. Automatic seismic damage identification of reinforced concrete columns from images by a region-based deep convolutional neural network. Struct. Contr. Health Monit. 26(3), e2313.

Yang, R.Y., Singh, S.K., Tavakkoli, M., et al., 2020. CNN-LSTM deep learning architecture for computer vision-based modal frequency detection. Mech. Syst. Signal Pr. 144, 106885.

Zhang, Q. Y., Barri, K., Babanajad, S.K. et al., 2020. Real-time detection of cracks on concrete bridge decks using deep learning in the frequency domain. Engineering. DOI: 10.1016/j.eng.2020.07.026.

Zhang, Y.Q., Miyamori, Y., Mikami, S., et al., 2019. Vibration-based structural state identification by a 1-dimensional convolutional neural network. Comp.-Aid. Civ. Infr. Eng. 34, 822-839.